ISSN 1810-2328, Journal of Engineering Thermophysics, 2018, Vol. 27, No. 1, pp. 58–71. © Pleiades Publishing, Ltd., 2018.

The Influence of Inlet Disturbances on the Post-Stall Behaviors in Compression System

W. Du[1*], X. Yunfeng[1], and G. Lorenzini[2***]**

[1] *Beijing Institute of Petrochemical Technology, Department of Engineering, Beijing, China*

[2] *Alma Universitas Studiorum Parmensis—University of Parma, Department of Engineering and Architecture, Parco Area delle Scienze, 181/A, Parma, 43124 Italy*

Received March 28, 2017

Abstract—The object of this paper is to provide a reliable tool to carry out the parametrical studies of post-stall behaviors in multistage axial compression systems. An adapted version of the 1.5D Euler equations with additional source terms is discretized with a finite volume method and are solved in time by a fourth-order Runge—Kutta scheme. The equations are discretized at mid-span both inside the blade rows and the non-bladed regions. The source terms express the blade-flow interactions and are estimated by calculating the velocity triangles for each blade row. Additional source terms are introduced to represent the effects of inlet disturbances on post-stall behaviors and the physical analysis is therefore proposed to explain the phenomenon.

DOI: 10.1134/S1810232818010071

INTRODUCTION

Dynamic simulations of post-stall transients are useful for design purpose and aero-thermodynamic analysis. The non-recoverable stall phenomenon gives strong motivations to analyze the post-stall behavior of the compression system in aeroengine field. The instabilities such as surge and rotating stall can cause the critical operating conditions and can generate high levels of mechanical constraints on compressor blades. Both the inlet total pressure obstructions and the inlet temperature spike due to flaming of fuel leakage can lead to the instability occurrence or significantly change the post-stall behavior in the multistage compression system. The experimental tests are difficult and expensive to study the influences of inlet disturbances during the design process. Therefore, numerical simulations become necessary to provide a reliable tool for designer to study the influence of inlet disturbances on the compression system, especially during the preliminary design phase.

This model is based on the solution of 1.5D axisymmetric Euler equation inside the turbomachinery. The mesh cells are not only distributed between blade rows, but also inside of each blade row, allowing for a detailed representation of the flow field. An adapted version of Euler equations including mass, meridional momentum, circumferential momentum and energy balances are applied for each control volume at mean radius. The source terms express the blade-flow interactions and are estimated by calculating the velocity triangles for each blade row [1, 2]. The external disturbances are considered in the source terms.

The current numerical tool has been validated the ability to capture the post-stall event in the Day's four-stage and Gamache's three-stage compression systems [3—5]. The test compressor rig of Day is still chosen as the test case to study the influence of inlet disturbances on post-stall behaviors. The numerical results are compared to observe the influences of inlet disturbances and the explanation is presented to analyze the physical mechanism. The results reveal that this tool has the ability to correctly reflect the influences of inlet disturbances on post-stall behaviors in multistage compression systems.

[*] E-mail: duwenhai@bipt.edu.cn

[**] E-mail: xiaoyunfeng@bipt.edu.cn

[***] E-mail: giulio.lorenzini@unipr.it

BACKGROUND

The compression system may experience the inlet disturbances during the engine operations, such as inlet total pressure obstructions or inlet temperature spike due to flaming of leakage fuel; therefore, further investigations should be carried out to study the effects of inlet flow disturbances on the post-stall event in the multistage axial compression system. The inlet total pressure distortion includes the radial distortion, the circumferential distortion and the combinations, which require 2D even 3D numerical tools when the flow mechanism is desired. During post-stall transient simulations, 2D or 3D models need very large computational resources because of the long length scale of multistage compression system and long time scale of operation procedure, like surge. Therefore, a simplification is made to focus on the overall effects of inlet obstructions rather than the detail flow field, which means that only the variations of total pressure along the axial direction are taken into account in the current simulations. In the real operations, the aero-engine may experience inlet flaming of leakage fuel during mid-air refueling process, which can lead to the inlet total temperature spike and may lower the surge margin, even change the post-stall event in the compression system [6]. Therefore, it becomes important to understand the influences of the inlet total temperature spike on the post-stall behaviors in compression system.

Parametric studies have been carried out to study the inlet disturbances by many researchers. Dirk studied the influence of inlet distortion on the instability inception of a low-pressure compressor [7]. Feng Lin researched the stall inception phenomenon in an axial compressor with inlet distortion [8]. Davis used stage-by-stage modeling technique to study the effects of inlet distortion screens, combustion instabilities, heat transfer due to rapid power-lever transients and possible stage hardware modifications [9]. Parametric studies were also carried out by Tauveron to study the local aspects, such as the effects of throttle setting and the adjustments of blade setting angle [10, 11].

In the current paper, the 1.5D model is applied to study the influence of inlet disturbances on surge cycle and surge frequency. The compressor rig of Day is implemented to validate the numerical results.

Model Description

It is assumed that the flow path meanline is a streamline and that the flow is axisymmetric. The fluid is treated as an ideal gas. The quasi-1.5D Euler equations are applied in a curvilinear (m, n, θ) coordinate system. The mass flow, meridional momentum, circumferential momentum and energy equations can be described in vector, nondimensional, conservative form, as follows:

$$\frac{\partial U}{\partial t} + \frac{\partial G}{\partial m} = Q, \tag{1}$$

$$U = \begin{bmatrix} \rho A \\ \rho V_m A \\ \rho r V_t A \\ \rho E^0 A \end{bmatrix}, \quad G = \begin{bmatrix} \rho V_m A \\ (P + \rho V_m^2) A \\ \rho r V_m V_t A \\ \rho H^0 V_m A \end{bmatrix}.$$

The source terms represented by Q in the Euler equations are used to represent the influence of the blade rows and the flow-path on the fluid. They can be split into four contributions: the isentropic action of the blades Q_b, the influence of friction Q_f, the influence of the flowpath geometry Q_g, and the external disturbance influences Q_{ex}, which have been shown in the reference papers [4, 5].

$$Q = Q_b + Q_f + Q_g + Q_{\text{ex}}. \tag{2}$$

Friction Source Term

In the Euler equations, the entropy production is due to a separate distributed friction force F_f in the momentum equations. This friction force is aligned with the relative velocity but has the opposite direction:

$$\overrightarrow{F_f} = -\left|\overrightarrow{F_f}\right| \frac{\overrightarrow{W}}{\left|\overrightarrow{W}\right|}. \tag{3}$$

The entropy production can be written as:

$$\rho T \frac{ds}{dt} = -\overrightarrow{W} \cdot \overrightarrow{F_f} \quad , \tag{4}$$

where $\overrightarrow{W}$ is the relative velocity vector. The magnitude of the friction force can be rewritten as:

$$F_f = \rho T \frac{W_m}{W} \frac{\partial s}{\partial x}. \tag{5}$$

Only the tangential component of the friction force can change the energy balance, and the friction source term can be described as following:

$$Q_f = \begin{bmatrix} 0 \\ F_{f,m} A \\ r F_{f,t} A \\ \Omega r F_{f,t} A \end{bmatrix}. \tag{6}$$

Blade Source Term

This term is implemented to represent the isentropic influence of blade rows. An angular momentum balance over a blade row provides the tangential component of the corresponding (inviscid) blade force $F_{b,t}$:

$$r(F_{f,t} + F_{b,t}) = \frac{q_m}{Vol} \Delta(r V_t). \tag{7}$$

It is intended that this force is applied in an isentropic way, the viscous contribution being applied separately through the friction source term. Therefore, this blade force is perpendicular to the relative velocity:

$$\overrightarrow{F_b} \cdot \overrightarrow{W} = 0. \tag{8}$$

Once again, only the tangential component of the blade force appears in the energy balance:

$$Q_b = \begin{bmatrix} 0 \\ F_{b,m} A \\ r F_{b,t} A \\ \Omega r F_{b,t} A \end{bmatrix}. \tag{9}$$

Geometry Source Term

This term represents the effect of the variation of the cross-section area and the meanline radius. The axial component can be derived as:

$$\frac{\partial \rho V_m A}{\partial t} + \frac{\partial (P + \rho V_m^2) A}{\partial x} = \frac{\rho A V_t^2}{r} \frac{\partial r}{\partial x} + P \frac{\partial A}{\partial x}. \tag{10}$$

This geometrical force does not contribute to the energy balance and also does not create entropy.

External Disturbances Source Term Inlet Total Pressure Obstructions

The inlet total pressure obstruction is usually implemented to study the effects of unfavorable flow patterns on the compression system. First, the viscous effects between the surfaces and the flow are represented by a friction force that is linearly distributed in the compressor inlet. The friction force can be represented as:

$$F_p = \left(\frac{k}{2} f P_s M^2 \right) \cdot \left(\frac{A}{2R} \right), \tag{11}$$

where f represents the total pressure loss due to the viscosity and inlet obstruction. Additional friction force is added inside certain control volumes at the inlet duct to represent the total pressure drop due to the inlet obstruction. Different f values are chosen according to the inlet obstruction and the variation of inlet total pressure is applied instantaneously in the paper. The direction of frictional force during the surge cycle is always in the opposite direction of the velocity.

Inlet Temperature Spike

The inlet temperature spike is introduced by changing the inlet temperature condition instantaneously.

Empirical Correlations

The accuracy of the simulations is highly dependent on the source terms in the equations, which are derived from empirical correlations, particularly loss coefficient and deviation angle models. Different empirical correlations have been chosen for entire flow conditions, such as a normal forward flow, stalled flow and reversed flow, and the current selected loss and deviation models can predict the satisfied performance results [3–5]. The separation of boundary layers in compressors has not been fully understood. In order to eliminate the uncertainty in numerical simulations, the stall inception and the stall recovery point of the Day's four-stage compressor are obtained from experimental results [12].

TRANSIENT SIMULATIONS

The time needed for stall cells to be fully developed can be several rotor revolutions and the mass flow undergoes significant changes during this time. The blade forces extracted from empirical correlations are steady and are not adequate for transient simulations. Therefore, a first-order time lag equation has been included in the model in order to provide the dynamic blade force [3]. It should be emphasized that only the axial force is modified. The shaft work, as well as the tangential force, is assumed constant.

$$\tau \frac{dF}{dt} + F = F_{ss}. \tag{12}$$

The time constant τ is approximated to be two rotor revolutions and will be kept constant in all transient simulations. The time lag equation is used only during rotating stall. The experimental observations suggest that the transition between rotating stall and reversed flow does not really occur at zero mass flow [13]. Thus, the time lag equation is applied until the flow coefficient reaches a value of -0.09; and the steady blade force is used during the rest of reversed flow. The flow range for the application of the time lag equations is shown in Fig. 1.

Parameter $B = \frac{U}{2a} \cdot \sqrt{V_p/(A_c L_c)}$ is used as a reference parameter proposed by Greitzer to determine whether rotating stall, surge or deep surge may occur in a particular compression system [14, 15].

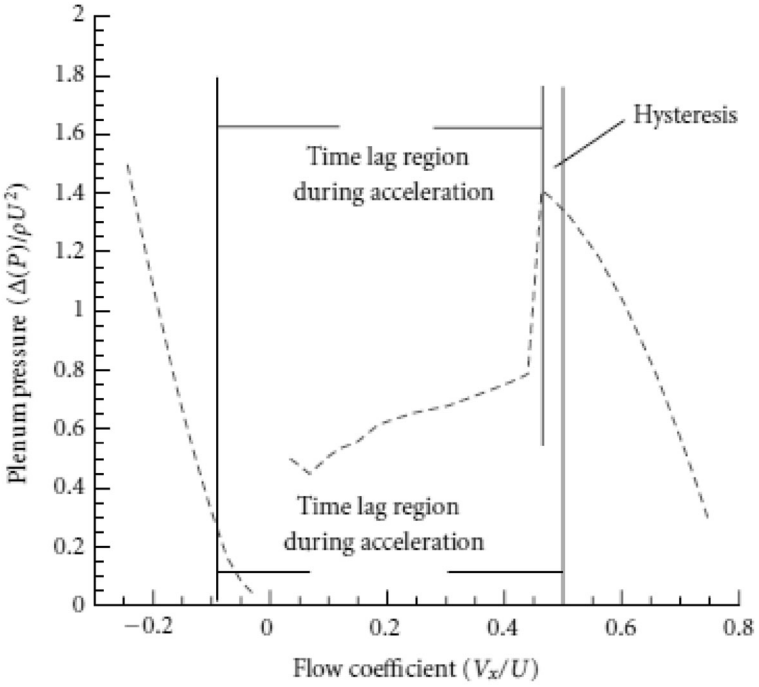

Fig. 1. Application of time lag for transient simulations.

NUMERICAL STUDIES

The four-stage compressor of Day is applied to study the influences of inlet disturbances. The post-stall behavior of the compression system is simulated and compared to the experimental results as showing in Fig. 2, which can be found in detail in previous studies [4].

Inlet Total Pressure Disturbances

In order to show the influence of inlet total pressure obstruction, the same four-stage compression system of Day, which is configured at $B = 0.67$, is used as the test compressor. The compression system exhibits a deep surge behavior at $B = 0.67$ as shown in Fig. 2. The total pressure distributions at inlet duct for different obstruction intensities are shown in Fig. 3. The effects of turbulent flow without inlet obstruction generates 0.8% total pressure loss, while turbulent effects plus two different inlet obstructions lead to 1.6% and 3.5% total pressure losses.

When the inlet pressure obstruction is implemented in the inlet duct, the throttle is gradually turned down to a critical position to just cause the compression system instability. Figure 4 shows the surge cycles for several obstruction test cases. It is found that the compression system exhibits deep surge cycles except for inlet pressure obstruction of 3.5%. The deep surge cycle is reduced when more inlet pressure loss is generated in the inlet duct. The total energy loss in the inlet duct weakens the ability of the compressor to recover from the stalled region. When the inlet pressure loss obstruction is more than 3.5%, the compressor cannot recover during the repressurization phase.

In order to study the different post-stall behaviors due to inlet pressure obstructions, the friction force in the inlet duct and the blade forces of each blade row are compared for two inlet pressure obstruction losses (1.6% and 3.5%). Figures 5 and 6 show the friction forces in the inlet duct and the blade forces of each blade at different time steps when inlet total pressure obstruction (1.6% and 3.5%) are, respectively, implemented in the numerical simulations. Four different time occurrences are selected to compare the friction forces and the blade forces. It can be found in Fig. 5 that the friction force is generally much smaller than the blade force, which indicates that the blade forces in the compressor are high enough to overcome the friction influence during the repressurization process. In Fig. 6, the friction forces due to the pressure obstruction in the inlet duct become of the same magnitude as the blade forces at different time steps, which weakens the compressor recovery ability and finally results in the non-recoverable operational condition.

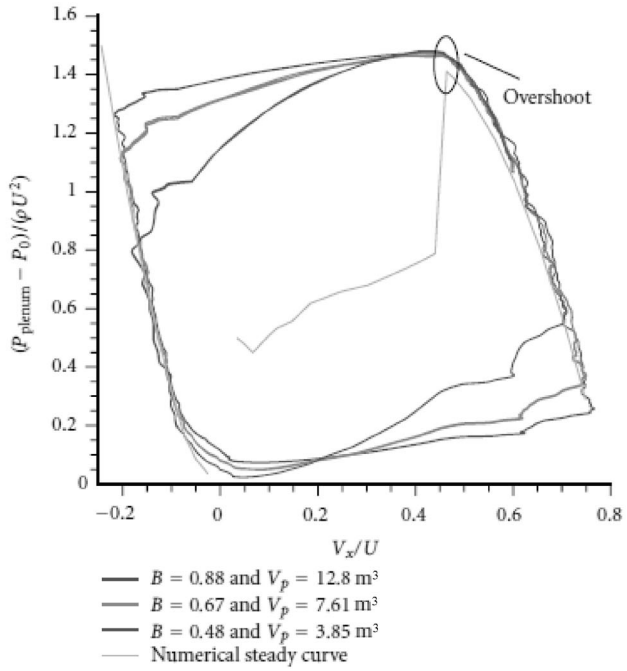

(a) Numerical performance characteristics during surge

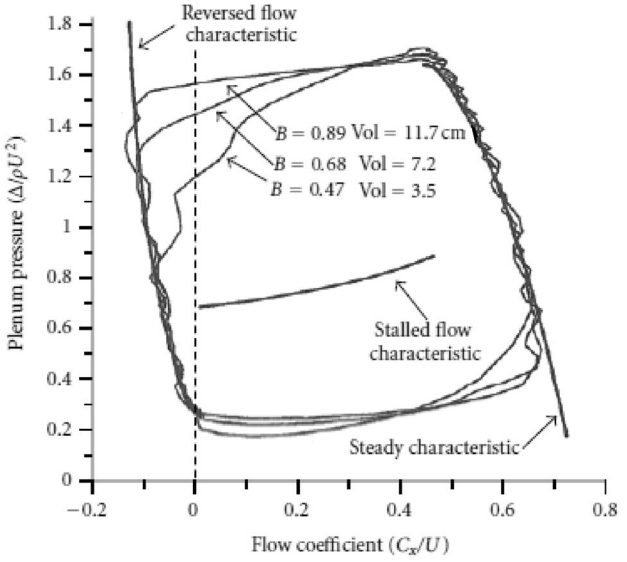

(b) Experimental performance characteristics during surge

Fig. 2. Numerical and experimental performance characteristics during surge of Day's four-stage compressor.

Inlet Total Temperature Spikes

The same compression system of Day at $B = 0.67$ is used to study the effect of total temperature spikes in the inlet duct. The compressor rotating speed and the throttle setting are fixed without the occurrences of rotating stall during the simulations. The inlet total temperature at the inlet duct is increased by 115.5 K, 216.5 K, and 288.1 K in the three numerical simulations after 25 rotor revolutions, by changing the inlet boundary condition.

Figure 7 shows the post-stall performances with three different inlet total temperature spikes. Figures 8 and 9 show the time history trajectories of the average mass flow coefficient and the pressure rise coefficient for the three different inlet total temperature disturbances. It is found that the compressor

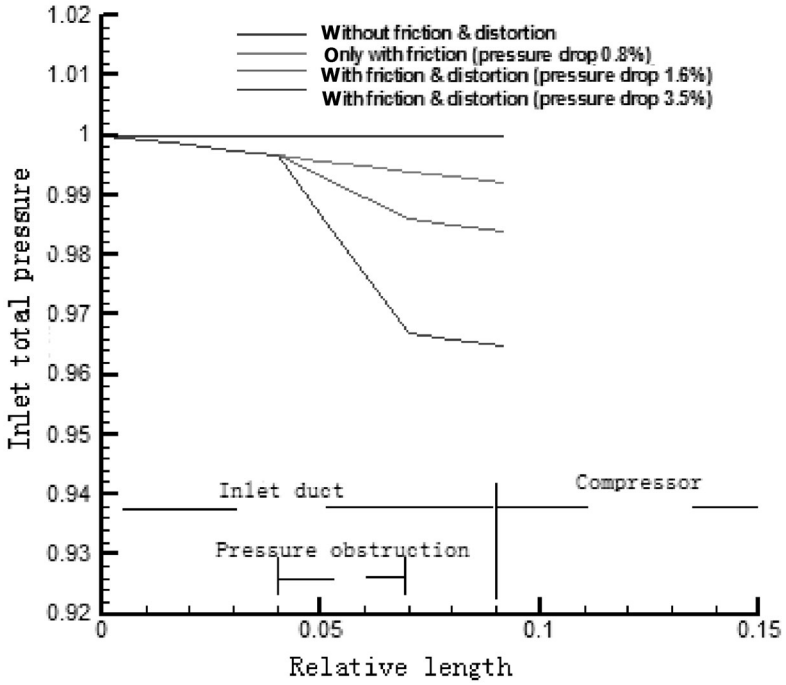

Fig. 3. Total pressure distribution in inlet duct for several numerical simulations.

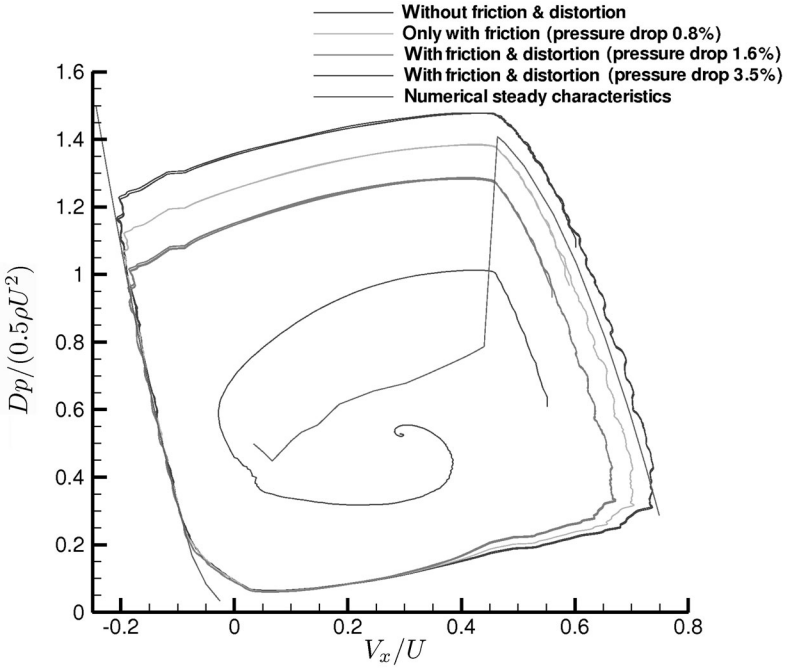

Fig. 4. Surge cycles comparisons in several numerical simulations at $B = 0.67$.

can directly operate in the stalled region due to an inlet total temperature spike, although the original compression system without inlet total temperature spike works at steady operating point. This indicates that the inlet total temperature spike can deteriorate the compression system surge margin.

Surge cycles become smaller when the inlet temperature spike is increased, and finally the compressor operates at a non-recoverable state after several surge cycles when the inlet total temperature spike

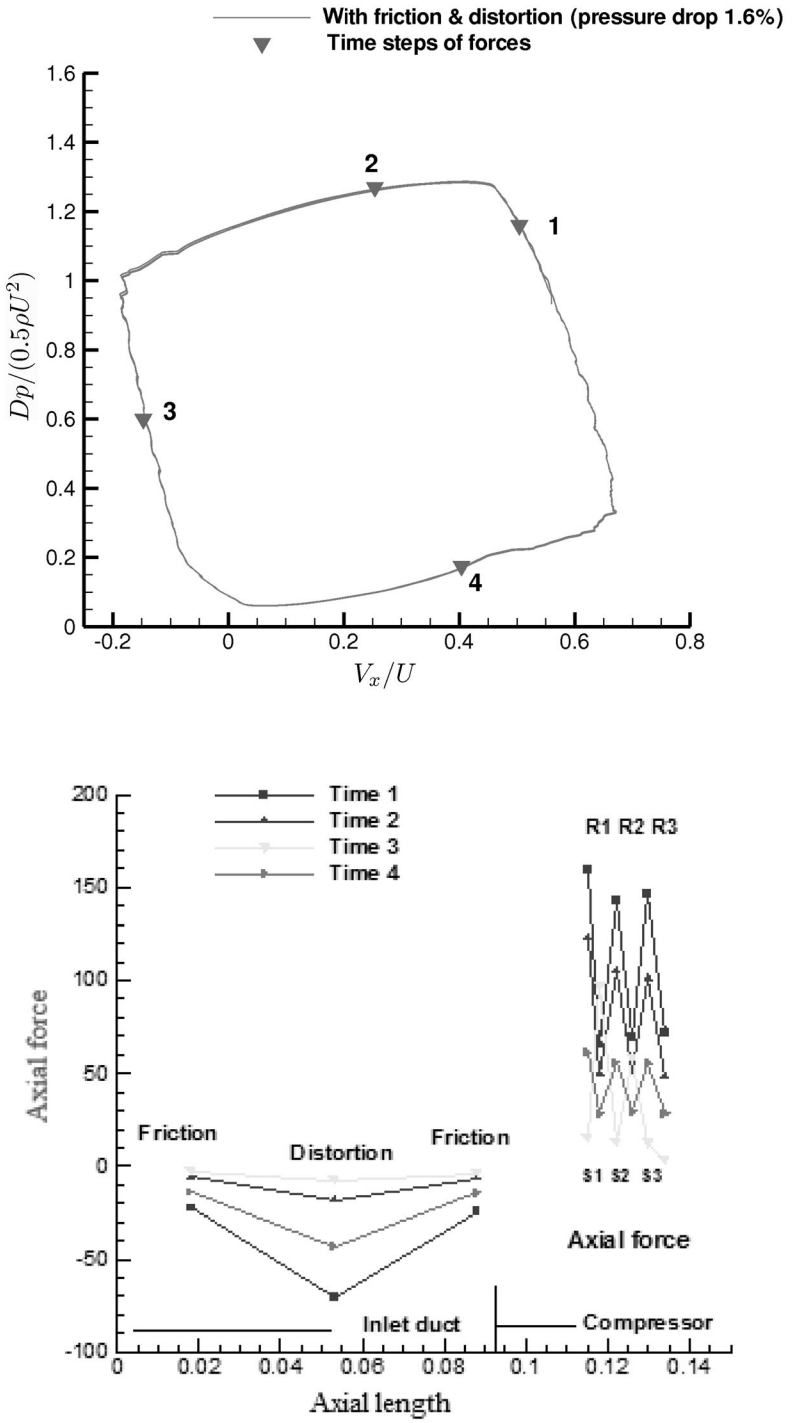

Fig. 5. Inlet friction forces and blade forces for pressure obstruction 1.6%.

is imposed to be 288.1 K. In Figs. 8 and 9, the compression system exhibits a damped pressure rise coefficient and mass flow coefficient with higher inlet total temperature spikes.

These numerical results show that the compression system exhibits non-recoverable stall conditions when high inlet temperature spikes are experienced. This phenomenon can be explained by the fact that an inlet total temperature spike leads to higher inlet temperatures for the compressor, thus effectively increases the sound speed. According to the definition of the Greitzer's parameter B, the compression system will operate at a smaller value of B when the inlet total temperature is increased [13, 14]. This

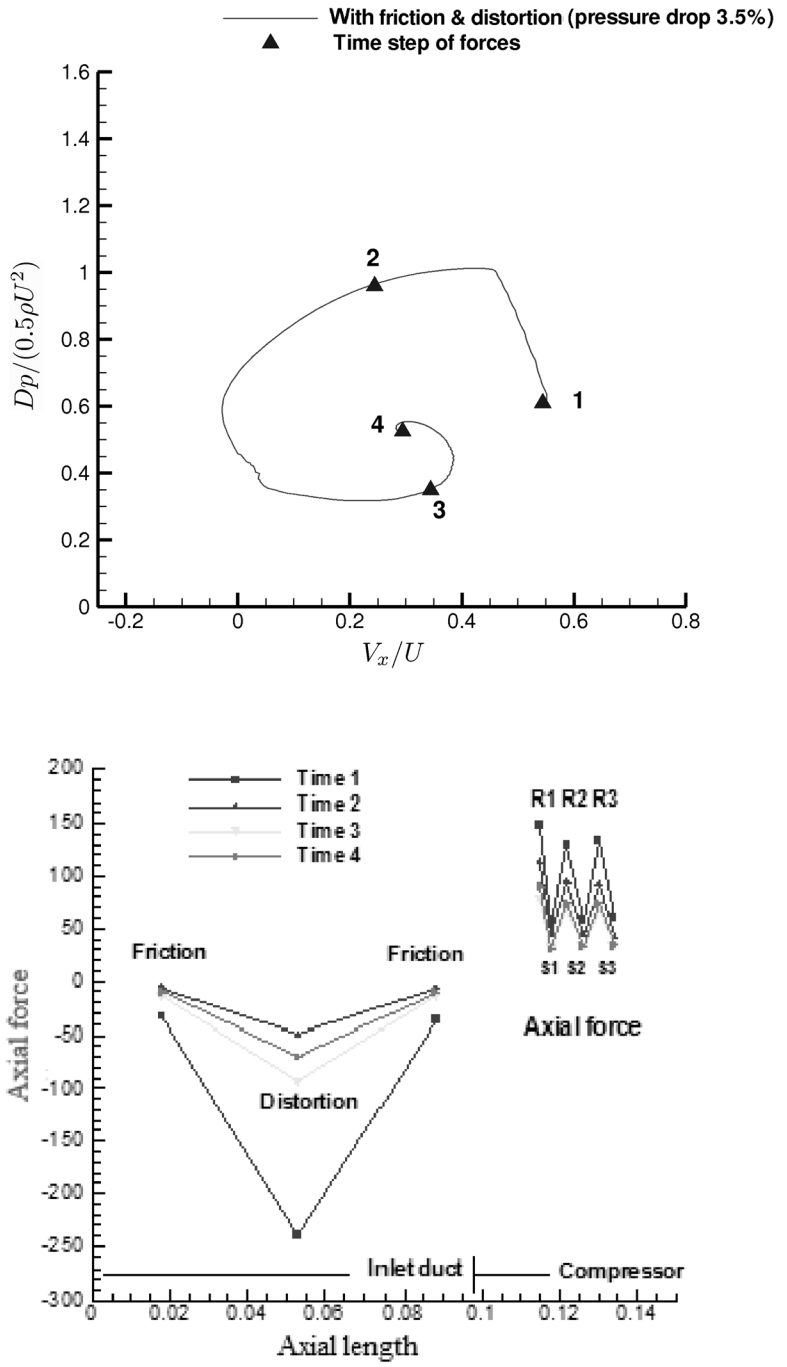

Fig. 6. Inlet friction forces and blade forces for pressure obstruction 3.5%.

is the reason why the compression system exhibits damped surge cycles when the inlet temperature is increased.

Figures 10 and 11 show the total pressure and total temperature distributions along the compressor with different inlet temperature spikes. It can be found that the total pressure rise is decreased when a high inlet temperature spike is experienced. This can be understood by the fact that the fluid becomes harder to be compressed with more energy. In Fig. 12, the surge frequencies are increased with higher inlet temperature spikes.

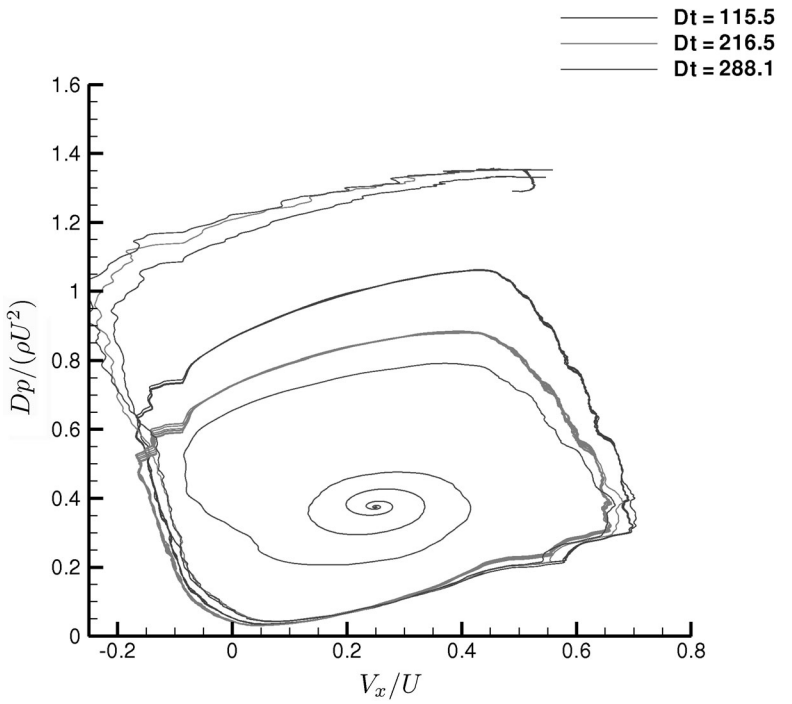

Fig. 7. Post-stall performances with different inlet temperature spikes.

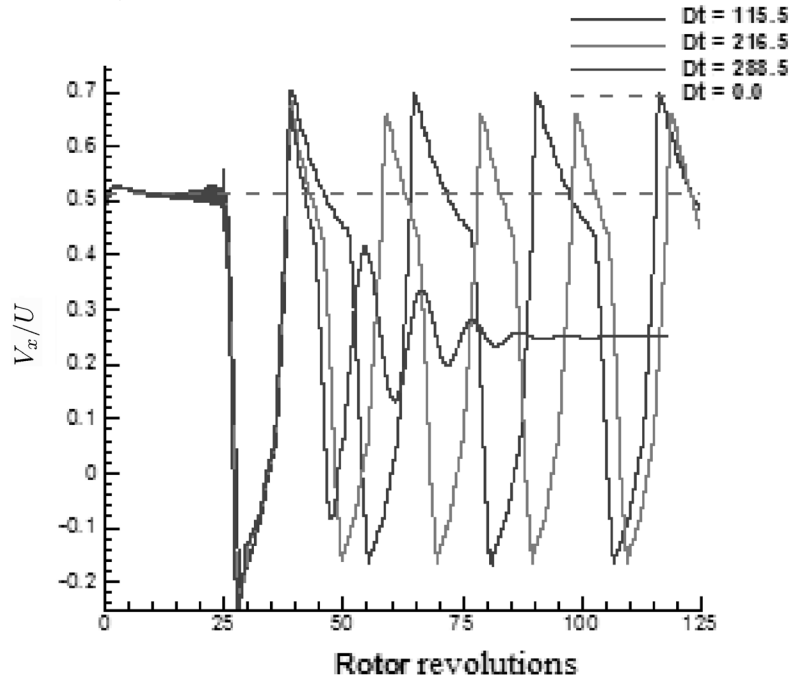

Fig. 8. Time history of mass flow coefficient with different inlet temperature spikes.

CONCLUSIONS

A reliable prediction tool has been developed and implemented to predict the influences of inlet disturbances on post-stall behavior of multistage compressor. The model is based on an adapted version of the 1D Euler equations with additional source terms, which are estimated by empirical correlations. The influences of inlet total pressure disturbances and inlet temperature spike are presented in the additional source terms.

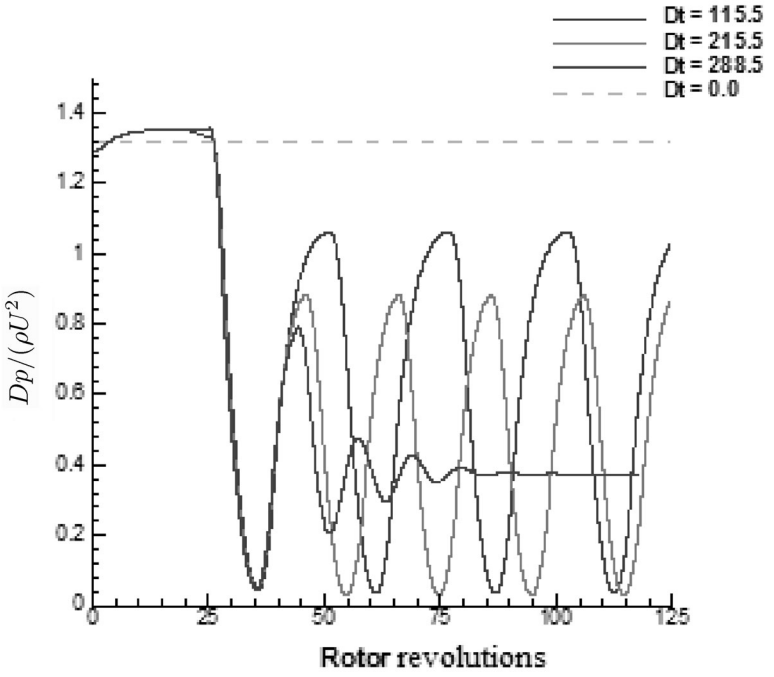

Fig. 9. Time history of pressure rise coefficient with different inlet temperature spikes.

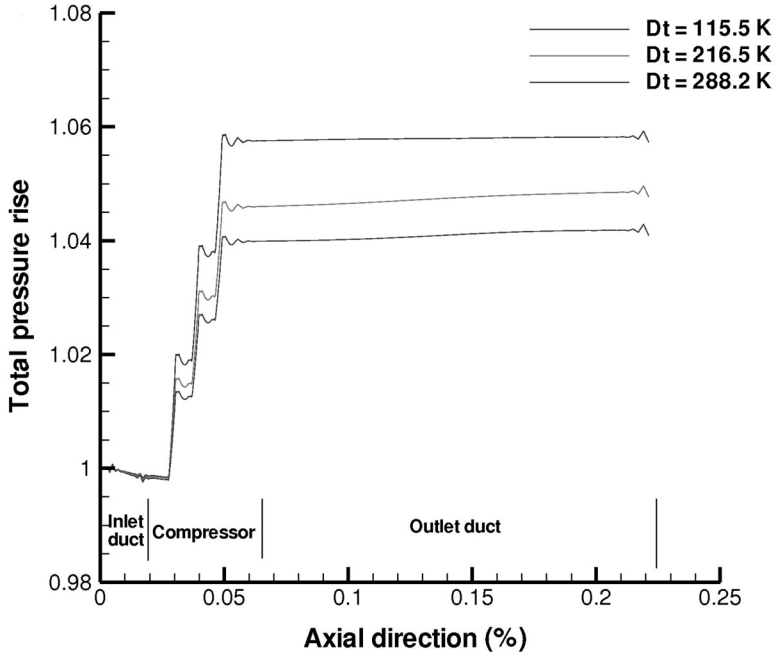

Fig. 10. Total pressure distributions inside compressor for different inlet temperature spikes.

This model can be used for preliminary design purpose as it is based only on the compressor geometry: the blade angles at mid-span and the hub and shroud geometry.

The compression system transits from deep surge to the non-recoverable condition when the inlet total pressure screen is instantaneously increased. This is probably due to the fact that the friction force in the disturbances region becomes equivalent to the blade force, thus the compressor achieves the non-

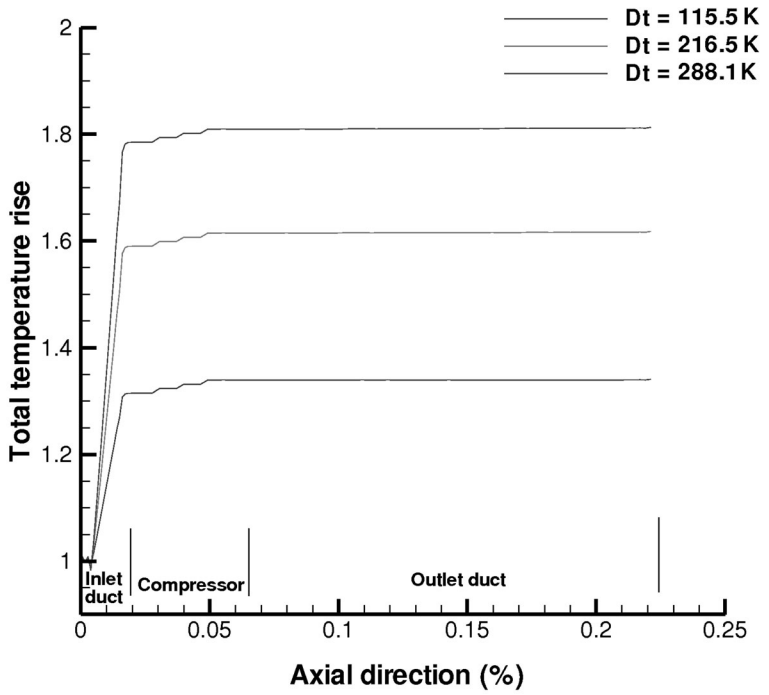

Fig. 11. Total temperature distributions inside compressor for different inlet temperature spikes.

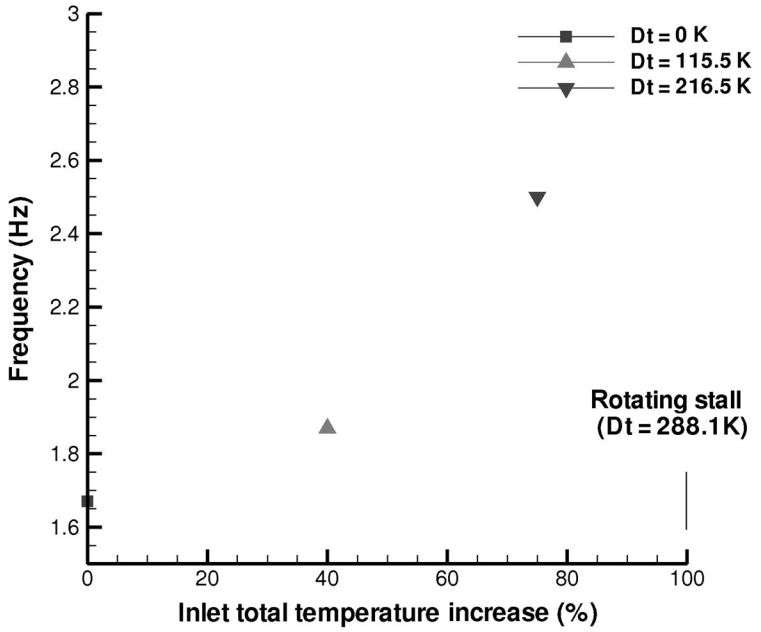

Fig. 12. Surge frequencies with different inlet temperature spikes.

recoverable condition during the acceleration process. Meanwhile, the inlet total pressure screen can reduce the surge oscillation due to the smaller surge excursions.

The inlet total temperature spike can deteriorate the surge margin of the compression system. Since the inlet total temperature spike can effectively lower parameter B, the numerical results show that the compression system exhibits a non-recoverable state with a higher inlet total temperature spike.

ACKNOWLEDGMENTS

The work was supported by the Beijing Municipal Natural Science Foundation, grant no. 3182009.

NOTATIONS

a—speed of sound

A—flow section area

B—non-dimensional number

Dp—pressure in plenum − ambient pressure

E—specific internal energy

F—force term

f—friction factor

H—specific enthalpy

i—incidence angle

k—constant value for friction force

L—effective length of equivalent duct

M—Mach number

P—pressure

Q—source term

r/R—radius

V, W—absolute and relative velocities

SW—shaft work

U—mean rotor velocity

V_p—exit plenum volume

ρ—density

Subscripts

0—ambient condition

m—meridional direction

t—tangential direction

p—plenum

c—compressor

s—static

Superscripts

0—total conditions

REFERENCES

1. Adam, O. and Léonard, O., A Quasi-One-Dimensional Model for Axial Compressor, *17th ISABE Conf.*, 2005.
2. Léonard, O. and Adam, O., A Quasi-One-Dimensional Model for Multistage Turbomachinery, *J. Therm. Sci.*, 2008, vol. 17, no. 1, pp. 7–20.
3. Wenhai, Du. and Léonard, O., A Quasi-One-Dimensional CFD Model for Multistage Compressors, *ASME*, pap. GT-2011-45497.
4. Wenhai, Du. and Léonard, O., Numerical Simulation of Surge in Axial Compressor, *Int. J. Rot. Machin.*, 2012, article ID 164831.
5. Du, W., Jun Qiang, Zh., and Léonard, O., Dynamic Simulations of Post-Stall Performance in Multistage Axial Compressors, *J. Therm. Sci.*, 2012, vol. 21, no. 4, pp. 1–11.
6. Crawford, R.A. and Burwell, A.E., Quantitative Evaluation of Transient Heat Transfer on Axial Flow Compressor Stability, *AIAA/SAE/ASME/ASEE, 21st Joint Propulsion Conf., AIAA*, Monterey, CA, 1985, pap. 85-1352.
7. Leinhos, D.C., Schmid, N.R., and Fottner, L., The Influence of Transient Inlet Distortions on the Instability Inception of a Low-Pressure Compressor in a Turbofan Engine, *J. Turbomach.*, 2000, vol. 123, no. 1, pp. 1–8.
8. Lin, F., Li, M., and Chen, J., Long-to-Short Length-Scale Transition: A Stall Inception Phenomenon in an Axial Compressor with Inlet Distortion, *J. Turbomach.*, 2005, vol. 128, no. 1, pp. 130–140.
9. Davis, M.W., A Stage-by-Stage Post-Stall Compression System Modeling Technique: Methodology, Validation, and Application, PhD Thesis, Virginia Polytechnic Institute and State University, 1987.
10. Tauveron, N., Saez, M., Ferrand, P., and Leboeuf, F., Axial Turbomachine Modeling with a 1D Axisymmetric Approach. Application to Gas Cooled Nuclear Reactor, *Nucl. Eng. Des.*, 2007, vol. 237, pp. 1679–1692.
11. Tauveron, N., Simulation Numérique et Analyse du Déclenchement et du Développement des Instabilités Axiales dans les Turbomachines. Application à un Transitoire de Brèche dans un Réacteur Nucléaire à Hélium, PhD Thesis, Ecole Centrale de Lyon, 2006.
12. Day, I.J., Axial Compressor Performance during Surge, *J. Propuls. Power*, 1994, vol. 10, no. 3, pp. 329–336.
13. Gamache, R.N. and Greitzer, E.M., Reverse Flow in Multistage Axial Compressors, *J. Propuls. Power*, 1990, vol. 6, no. 4, pp. 461–473.
14. Greitzer, E.M., Surge and Rotating Stall in Axial Flow Compressors, Part I: Theoretical Compression System Model, *J. Eng. Power*, 1976, vol. 98, no. 2, pp. 190–198.
15. Greitzer, E.M., Surge and Rotating Stall in Axial Flow Compressors, Part II: Experimental Results and Comparison with Theory, *J. Eng. Power*, 1976, vol. 98, no. 2, pp. 199–211.